Available online at www.sciencedirect.com
SCIENCE DIRECT®
Journal of Sound and Vibration 278 (2004) 117–134
JOURNAL OF SOUND AND VIBRATION
www.elsevier.com/locate/jsvi

A comparison of two methods of simulating seat suspension dynamic performance

T.P. Gunston[a], J. Rebelle[b], M.J. Griffin[a,*]

[a] *Human Factors Research Unit, Institute of Sound and Vibration Research, University of Southampton, Highfield, Southampton SO17 1BJ, UK*

[b] *Centre de Recherche de Nancy, Institut National de Recherche et de Sécurité, Avenue de Bourgogne, BP 27, 54501 Vandoeuvre, France*

Received 2 September 2002; accepted 29 September 2003

Abstract

Many off-road machines are equipped with a suspension seat intended to minimize the vibration exposure of the operator to vertical vibration. The optimization of the isolation characteristics of a suspension seat involves consideration of the dynamic responses of the various components of the seat. Ideally, the seat components would be optimized using a numerical model of the seat. However, seat suspensions are complex with non-linear characteristics that are difficult to model; the development of seat suspensions is therefore currently more empirical than analytical. This paper presents and compares two alternative methods of modelling the non-linear dynamic behaviour of two suspension seats whose dynamic characteristics were measured in the laboratory. A 'lumped parameter model', which represented the dynamic responses of individual seat components, was compared with a global 'Bouc–Wen model' having a non-linear degree-of-freedom. Predictions of the vibration dose value for a load placed on the seats were compared with laboratory measurements. The normalized r.m.s. errors between the predictions and the measurements were also determined. The median absolute difference between the measured and predicted seat surface vibration dose values over all test conditions for both models was less than 6% of the measured value (with an inter-quartile range less than 20%). Both models were limited by deficiencies in the simulation of top end-stop impacts after the load lifted from the seat surface. The lumped parameter model appears best suited to the development of the overall design of a suspension seat. The Bouc–Wen model can provide a useful simulation of an existing seat and assist the optimization of an individual component in the seat, without measuring the dynamic properties of components in the seat except those of the component being optimized.
© 2004 Elsevier Ltd. All rights reserved.

*Corrresponding author. Tel.: +44-023-8059 2277; fax: +44-023-8059 2927.

E-mail addresses: t.p.gunston@soton.ac.uk (T.P. Gunston), jerome.rebelle@inrs.fr (J. Rebelle), m.j.griffin@soton.ac.uk (M.J. Griffin).

0022-460X/$ - see front matter © 2004 Elsevier Ltd. All rights reserved.
doi:10.1016/j.jsv.2003.09.063

1. Introduction

Suspension seats are used to lessen the vibration transmitted from the floor of some vehicles to the operator. A new seat, or a modified existing seat, must undergo standardized laboratory tests with human subjects in order to be passed as suitable for sale [1–3]. The testing is time-consuming and costly and does not indicate what changes would improve the dynamic performance of the seat.

Mathematical models of suspension seats allow seat behaviour to be investigated without laboratory testing. Various non-linear theoretical models of suspension seats have been described [4–12]. The majority of these models have used a lumped parameter approach to describe the seat by coefficients related to specific component parts and then solved the resulting equations, some of them non-linear, using numerical integration techniques. The complexity of suspension seat models has progressively increased by including more detailed descriptions of the seat components. The first model described in this paper, referred to as the 'lumped parameter' model, continues this approach.

In the second model used here, referred to as the 'Bouc–Wen' model, the dynamic characteristics of the seat suspension and cushion were described using a Bouc–Wen formula [13,14]. The Bouc–Wen coefficients were obtained by minimizing the difference between the predicted and measured accelerations of a load supported in the seat. This approach allows parameters to be determined for an existing seat from a few laboratory measurements, rather than by measuring the dynamic characteristics of each component individually.

The first objective of this study was to quantify the prediction performance of the two alternative methods of modelling suspension seats designed for off-road vehicles. The second objective was to compare the strengths and weaknesses of the alternative models and identify their potential applications.

2. The seats

Two suspension seats in current production were used for this investigation. One seat was a compact design for use in industrial trucks (e.g., fork lift trucks) with the suspension components mounted behind the backrest (Fig. 1). The other seat was designed for use in earthmoving

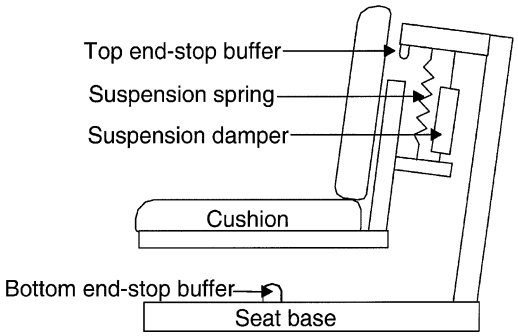

Fig. 1. Schematic of the industrial truck seat.

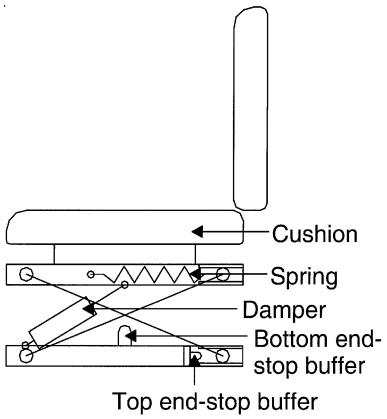

Fig. 2. Schematic of the earthmover seat.

machinery with the suspension components mounted under the seat cushion (see Fig. 2). Both seats had covered foam cushions, steel coil springs, oil dampers and rubber end-stop buffers. The seats are considered representative of seats mounted on many off-road machines. The design of seats mounted on tractors, earthmovers, industrial trucks and forwarders are similar and consist of a suspension (springs, damper, guiding system), a cushion, and two sets of end-stop buffers, one to limit the free upward travel and the other to limit the downward travel.

3. The models

3.1. The lumped parameter model

3.1.1. Overview

The lumped parameter model used in this study is shown schematically in Fig. 3. The model employs the dynamic properties of the component parts and therefore required separate dynamic measurements of each of the components. The following sections summarize the measurements used to describe the seat components by parameters in the model. The parameter values used to describe the two seats are listed in Appendix A. The equations describing each component are reported elsewhere [11] and were solved by numerical integration using a fourth order Runga–Kutta algorithm.

3.1.2. The cushion

The cushions were described by a parallel linear spring and damper element with a restriction that the force applied by the cushion to the load mass was limited to a minimum of $-m_o g$, where m_o is the load mass in kg and g is the acceleration due to gravity. By this arrangement, the downward force on the load was not in excess of that due to gravity. The gravitational force acting on the remaining masses was accounted for by the assumed preload force acting on the suspension springs in order to set the suspension to the desired ride position.

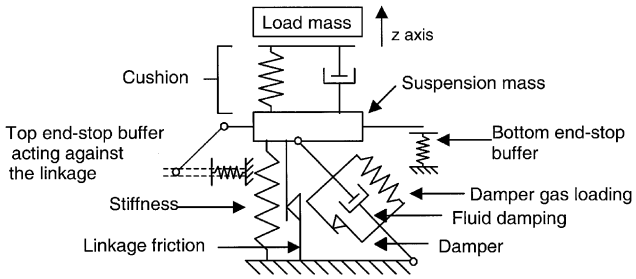

Fig. 3. Schematic of the lumped parameter model.

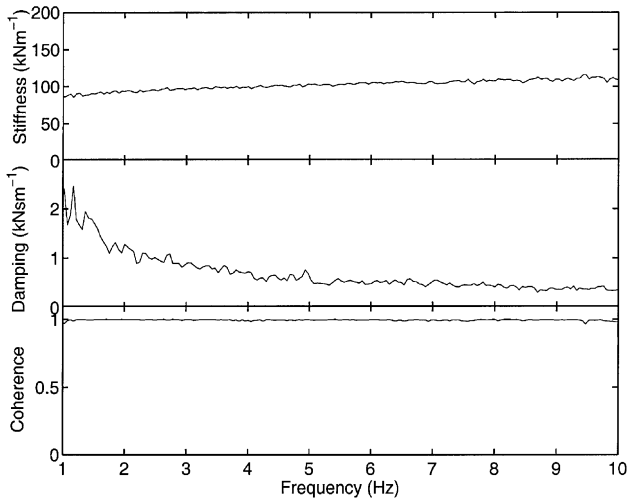

Fig. 4. Estimated cushion stiffness and damping for the earthmover seat cushion obtained by indenting the cushion with a 500-N static force and measuring the cushion apparent mass in response to a random flat acceleration spectrum test motion.

The cushions were preloaded to 500 N using a fixed circular indenter plate of 250-mm diameter [15] and subjected to random vertical vibration band-limited at 1 and 10 Hz. The applied acceleration and transmitted force were measured and converted to estimates of the cushion linear stiffness and damping using the following equations, derived from Ref. [16]:

$$k_c(\omega) = -\mathrm{Re}(m_c(\omega))\omega^2, \tag{1}$$

$$c_c(\omega) = -\mathrm{Im}(m_c(\omega))\omega, \tag{2}$$

where k_c is the cushion stiffness, c_c is the cushion damping, and m_c is the cushion apparent mass. The estimated cushion stiffness, damping and coherency of the earthmover seat cushion are shown in Fig. 4. The stiffness and damping at 2 Hz were used in the model. This frequency was chosen as being typical for the dominant vertical cabin floor vibration in wheeled on- and off-road vehicles to which suspension seats are often fitted.

3.1.3. The suspension linkage and stiffness

The suspension mechanisms were subjected to a quasi-static force–deflection test with the cushion and suspension damper mechanism removed. The suspension linkage force-deflection characteristic for the earthmover seat suspension is shown in Fig. 5. The suspension linkage friction was initially estimated as half the mean difference between the force in compression and the force in extension over the free travel region between the end-stop buffers. The effective vertical suspension spring rate was estimated as the mean gradient over the same region.

3.1.4. The suspension damper

The damper force–velocity characteristic was described in terms of a two-stage third order polynomial as shown in the following equations. Friction forces from the damper and the suspension linkage were modelled as constant forces opposing the motion or as a force just sufficient to prevent motion if the acting force was insufficient to overcome the friction force. Both force–velocity and friction forces were defined by separate coefficients for compression and extension and account was taken of the change in damping force with displacement due to the angled damper mounting in the earthmover seat.

$$F_1 = c_1\dot{z} + c_2\dot{z}^2 + c_3\dot{z}^3|_{\dot{z}<\dot{z}_1}, \tag{3}$$

$$F_2 = c_4(\dot{z} - \dot{z}_1) + c_5(\dot{z} - \dot{z}_1)^2 + c_6(\dot{z} - \dot{z}_1)^3 + c_1\dot{z}_1 + c_2\dot{z}_1^2 + c_3\dot{z}_1^3|_{\dot{z}\geqslant\dot{z}_1}, \tag{4}$$

$$F_d = F_1 + F_2, \tag{5}$$

where $\dot{z}$ is the relative velocity across the damper along the damper axis, F_d is the damping force and $\dot{z}_1$ is the velocity at which the damper changes between the polynomial described by coefficients c_1, c_2, c_3 and that described by coefficients c_4, c_5, c_6.

The friction forces and damper force–velocity characteristics were estimated from the dynamic response of the seat during the laboratory tests as described elsewhere [17]. A simple downhill

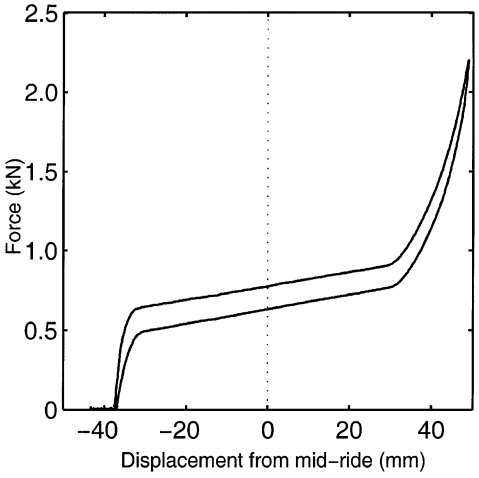

Fig. 5. Suspension force–deflection characteristic for the earthmover seat suspension obtained with the cushion and damper removed from the seat and the preload as set for the mid-ride position with the anthropodynamic dummy on the seat.

search algorithm was used to apply a multiplier to the measured friction and force–velocity functions in order to minimize the r.m.s. error between the measured and predicted seat load acceleration time histories. One test condition that did not result in end-stop impacts was used to estimate the friction coefficients, and one condition involving end-stop impacts was used to estimate the force–velocity characteristic. Both motions had a frequency of 2.25 Hz with the waveform shapes shown in Fig. 10 (see below) and magnitudes as shown in Table 1. The values for the friction and force–velocity coefficients obtained using this optimization process are shown in Table 2.

3.1.5. The end-stop buffers

The end-stop buffers were described as non-linear stiffness elements in terms of fifth order polynomial functions. The coefficients of these polynomials were determined by applying a least-squares curve fit to the measured buffer force–deflection characteristics. The use of this comparatively high order fit resulted in simulated force–deflection characteristics that were within 1% of the measurements over the range of compressions for which results were available (i.e., 5-mm compression of the top buffer resulting in a 6-kN force, and 15-mm compression of the bottom buffer resulting in a 450-N force). The measured force–deflection characteristics for the bottom buffers are shown in Fig. 9.

3.2. The Bouc–Wen model

3.2.1. Seat suspension model—assumptions

The Bouc–Wen model used in this study is shown schematically in Fig. 6.

Table 1
Seat base accelerations of the 2.35-Hz motions used to optimize the suspension damping parameters expressed in terms of r.m.s. acceleration and W_k-weighted VDV

	Motion used to optimise the friction coefficients (no end-stop impacts)		Motion used to optimise the damper force–velocity coefficients (end-stop impacts occurred)	
	r.m.s. accel	VDV	r.m.s. accel	VDV
Earthmover seat	1.82 m/s^2	1.62 $m/s^{1.75}$	3.83 m/s^2	3.42 $m/s^{1.75}$
Industrial truck seat	0.89 m/s^2	0.78 $m/s^{1.75}$	1.84 m/s^2	1.63 $m/s^{1.75}$

Table 2
Optimal gains for the suspension damping coefficients as determined by the optimization process

	Gain applied to the friction coefficients	Gain applied to the damper force–velocity characteristic coefficients
Earthmover seat	0.61	0.70
Industrial truck seat	1.36	0.85

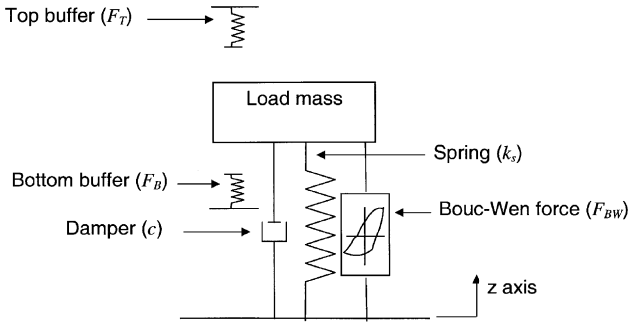

Fig. 6. Schematic of the Bouc–Wen model.

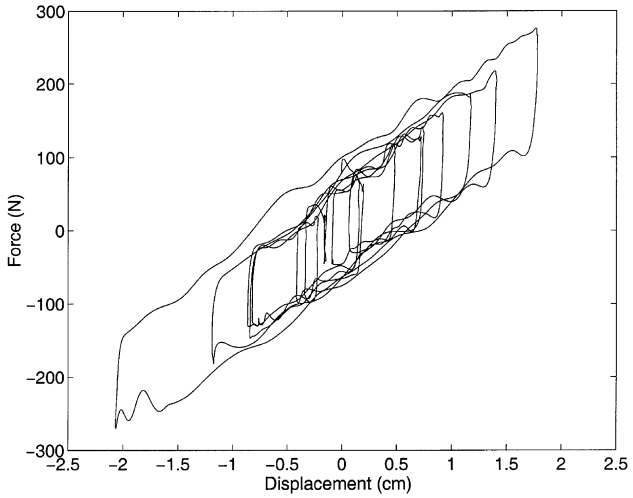

Fig. 7. Force-displacement diagram—industrial truck seat exposed to random excitation.

To limit the number of parameters needed to model the behaviour of the seat, a global approach was used, based on the measured input motion (acceleration, relative velocity or relative displacement) at the seat base and the measured output motion (acceleration, relative velocity or relative displacement) on the seat cushion.

Fig. 7 shows a typical hysteretic behaviour of the industrial truck seat measured with random excitation in the frequency range 0.5–5 Hz, which included the seat resonance frequency.

The Bouc–Wen model describes a wide variety of hysteretic systems [14]. The friction force $F_{BW}(t)$ is related to the relative vertical displacement $z(t)$ of the suspension according to the first order non-linear differential equation:

$$\dot{F}_{BW}(t) = (k - k_s)\dot{z} - \gamma|\dot{z}|F_{BW} - \beta\dot{z}|F_{BW}|, \tag{6}$$

where k and k_s are positive stiffnesses and where γ and β give the effect of the hysteresis. This model was first proposed by Bouc in 1967, then generalized and applied to structures exposed to earthquake excitation [13,18] and has subsequently been used for other applications.

A non-linear single-degree-of-freedom vertical seat suspension with hysteresis can be modelled by two equations:

$$M\ddot{z} + c\dot{z} + k_s z + F_{BW} + F_T + F_B = -M\ddot{\Phi},$$
$$\dot{F}_{BW} = (k - k_s)\dot{z} - \gamma|\dot{z}|F_{BW} - \beta\dot{z}|F_{BW}|, \tag{7}$$

where $z(t)$ is the vertical relative displacement of the suspension, $F_{BW}(t)$ is the previously defined Bouc–Wen force, M is the mass, c is the viscous damping coefficient (assumed to be linear), k_s is the stiffness of the suspension, and $\ddot{\Phi}(t)$ is the input excitation. F_T and F_B represent the reaction force of the top end-stop buffers (8) and the bottom end-stop buffers (9). All the non-linear effects due to the different seat components are combined in the $F_{BW}(t)$ force. The term $M(m_1 + m_{mm})$ represents the inert mass placed on the cushion (m_1) and the mass of the moving mass of the seat suspension (m_{mm}). Both masses are assumed to be rigidly fixed to the seat suspension. Consequently, five parameters must be identified to describe the suspension behaviour (when there is no impact on the end-stop buffers): c, k_s, k, γ and β.

The top end-stop buffers were modelled simply as an equivalent buffer (i.e., a soft linear spring–damper, c_1, k_1, system) which produces an equivalent reaction force, F_T, when the suspension exceeds its mid free-travel (d). The relative motion between the inert mass and the seat cushion were neglected. The inert mass was considered as fixed to the seat suspension model. This relative displacement was taken into account in the equivalent top buffer model so as to describe the acceleration time histories measured on the mass (see Section 3.2.2.2: "*Top buffers*").

$$F_T = k_1(z - d) + c_1\dot{z}, \quad z > d. \tag{8}$$

The bottom buffers were modelled as a cubic non-linear stiffness ($k_1; k_3$):

$$F_B = k_1(z + d) + k_3(z + d)^3 \quad z < -d. \tag{9}$$

3.2.2. *Identification of the parameters*

The parameters of the Bouc–Wen seat model were identified in two steps. Firstly, the suspension model parameters were obtained by means of curve fitting using the output acceleration time histories measured with no end-stop impacts. Secondly, the end-stop buffer model parameters were identified by curve fitting using the static force–deflection curves for the bottom buffer and using output acceleration measurements for the equivalent top buffer.

3.2.2.1. Identification of the seat suspension model parameters. The test seats were mounted on an hydraulic shaker platform and excited by imposed random displacement signals over a frequency range from 0.5 to 5 Hz. The excitation was generated during 16 s and included high and low levels of displacement in order to generate all the seat behaviour phases: stick-slip phases and free motion. The absolute input acceleration was measured on the shaker platform. The relative output displacement and the absolute acceleration of the seat were also measured. Data acquisition started with a zero level, for a few seconds, to fulfil null initial conditions in the numerical integration of the dynamic equations. The industrial truck seat was loaded with a 45-kg mass and the earthmover seat with a 58-kg mass (m_1). The masses of the moving parts of the two seats were estimated at about 13.5 and 27 kg, respectively (m_{mm}). The total load mass, M, was therefore equal to 58.5 and 85 kg.

The identification procedure was based on an optimization method [19,20] minimizing the quadratic error between the measurement and the numerical solution. The latter was obtained by the fourth order Runge–Kutta method. The parameter values obtained are given in Table 3.

In order to converge towards the optimal set of parameter for the seat suspension model, several optimizations were performed using different types of input excitation and different sets of initial value. The optimal set of parameter was obtained by calculating the average for each parameter from each optimization procedure. The parameters k_s, k and c are first order parameters and are unique. On the other hand, the parameters γ and β are second order parameters and several couples of value can exist. An example of the fit obtained from this calculation for the industrial truck seat is shown in Fig. 8.

3.2.2.2. Identification of the end-stop buffer model parameters. Bottom buffers: The damping of the nominal bottom buffers was neglected. The end-stop buffers were modelled as a pure non-linear stiffness. The static force–deflection curves of the bottom buffers shown in Fig. 9 were used to identify, by curve fitting, the model parameters given in Eq. (9): k_1 and k_3.

The values of k_1, k_3 and c_1 are reported in Table 4.

Top buffers: The aim was not to describe the real behaviour of the top buffers but to predict the acceleration peaks on the load when top impacts occurred. Consequently, the relative displacement of the mass during the impact phases was not well described because the mass

Table 3
Calculated parameter values of the seat suspensions

	k_5 (N/m)	k (N/m)	γ (m^{-1})	β (m^{-1})	c (N s/m)
Industrial truck	8156	3 20 897	94 371	−83 727	301.3
Earthmover	7502	2 40 640	93 226	−85 103	737.1

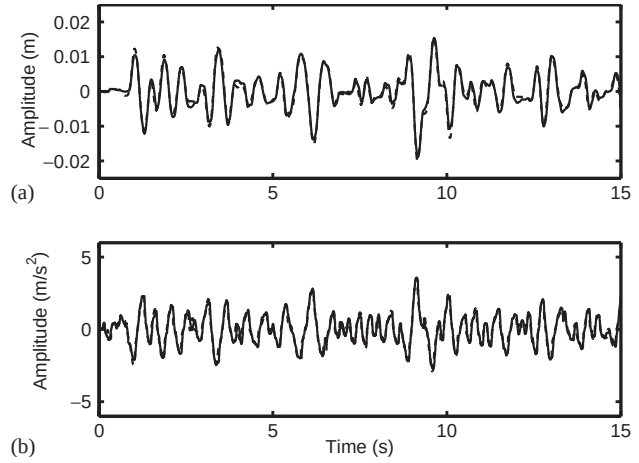

Fig. 8. Motion of the industrial truck seat loaded with a 45-kg mass (m_1) showing (a) the relative suspension displacement and (b) the absolute seat surface acceleration; —, measured; - - -, estimated.

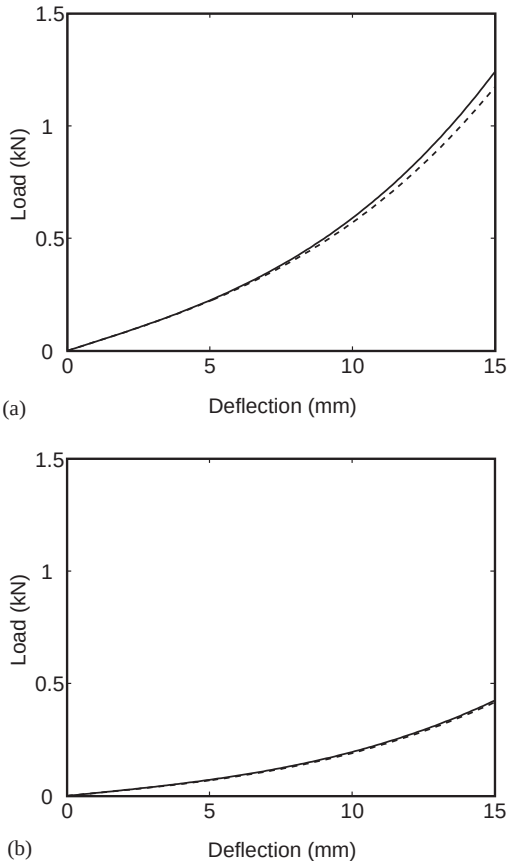

Fig. 9. Bottom buffer force-deflection curves for (a) the industrial truck seat and (b) the earthmover seat; —, measurement; - - -, model.

Table 4
Parameter values of top and bottom buffer models (Eqs. (8) and (9))

	Bottom buffer		Top buffer	
	k_1 (N/m^1)	k_3 (N/m^3)	c_1 (N s/m^1)	k_1 (N/m^1)
Industrial truck	80 000	3.4E8	200	9000
Earthmover	25 020	1.46E8	0	6000

was considered fixed to the seat. In practice, during high impacts, the mass was not always in contact with the seat cushion. The parameters of the equivalent impact force, F_T, were identified by fitting the whole model to the output acceleration response when impacts occurred. During this identification, all the seat parameters, including those of the bottom buffers, were kept at their previously identified values. Top buffer parameter values, c_1 and k_1, were optimized from Eq. (7). Table 4 gives the calculated values of the top and bottom buffer parameters.

From the calculated result, the equivalent top buffers appeared to be soft, whereas their physical behaviour was found by experiment to be relatively stiff (in the static force–deflection curve). This arose because the relative displacement between the inert mass and the seat cushion was neglected in the seat suspension system but was taken into account within an equivalent top buffer model. Further consideration of this model has been presented elsewhere [12].

4. Experimental procedure

4.1. Laboratory seat tests

The earthmover suspension seat and the industrial truck suspension seat were tested in the Human Factors Research Unit laboratory at the Institute of Sound and Vibration Research using a 58-kg rigid load on the seats. The seats were exposed to three transient vibrations, having different fundamental frequencies, derived from vehicle cab floor motions measured in off-road vehicles when, for example, a vehicle passes over an obstacle [21]. Such an excitation may cause impacts with the seat end-stop buffers. The acceleration waveform reproduced at the base of the seat using an electro-hydraulic vibrator is shown in Fig. 10. The motion was reproduced with fundamental frequencies of 2.1, 2.35 and 3.25 Hz, chosen as being close to the peak of the power spectrum for the simulated vibration seat tests in current standards, as listed in Table 5.

The seats were mounted on the electro-hydraulic vibrator capable of ± 500 mm and ± 10 m/s^2. A seat index point device, as specified in ISO 5353 [22], was used as the seat load. It was placed on the seat cushion and ballasted to 58 kg using rigidly attached steel blocks. An inert load was assumed to be an adequate first approximation to the human body due to the low frequencies used in the tests. It was considered preferable to compare the non-linear simulations with the laboratory measurements of the seat response without the variability inherent in tests with human subjects. The load was placed on the seat at least 5 min before any measurements were taken. The seat adjustment for driver mass was set so the mean ride position of the seat suspension was at the

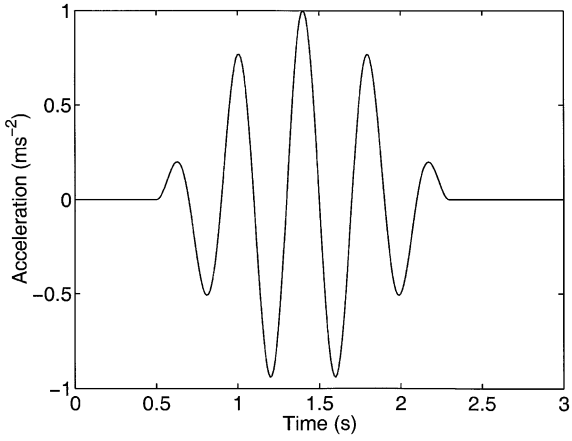

Fig. 10. The input motion used to measure the dynamic performance of the two seats.

Table 5
The approximate frequencies corresponding to the peak acceleration power spectra of standardized vibrations used for suspension seat testing

Approximate frequency of the acceleration power spectrum peak value (Hz)	Standard vibration test	Intended vehicle
2.1	ISO 7096 [2] EM2	Scraper without suspension
	ISO 7096 [2] EM3	Wheel loader
	ISO 7096 [2] EM4	Grader
	ISO 7096 [2] EM5	Wheel dozer, wheeled soil compactor, backhoe loader
	prEN 13490 [3] IT4	All terrain industrial trucks
	prEN 13490 [3] IT3	Industrial trucks above 9000 kg
2.35	ISO/CD 5007 [1] Class 2	Agricultural tractor of between 3600 and 6500 kg unballasted mass
3.25	prEN 13490 [3] IT2	Industrial trucks between 3500 and 9000 kg

Table 6
The range of input magnitudes in terms of W_k frequency-weighted VDVs

Frequency (Hz)	Earthmover seat		Industrial truck seat	
	Lowest magnitude ($m/s^{1.75}$)	Highest magnitude ($m/s^{1.75}$)	Lowest magnitude ($m/s^{1.75}$)	Highest magnitude ($m/s^{1.75}$)
2.1	0.81	3.30	0.43	1.85
2.35	0.86	4.20	0.44	1.96
3.25	1.05	8.05	0.47	5.23

mid-point of the available free travel between the end-stop buffers. A 5-Hz sinusoid with a displacement of ± 1 mm was applied to overcome suspension friction after adjusting the control for driver mass.

The acceleration at the base of the seat and at the base of the load were measured using Entran EGCSY-240D-10 accelerometers; the displacement of the seat suspension relative to the vibrator platform was measured using an RDP DCT4000C LVDT. The signals from the transducers were acquired digitally at 512 samples/s using an *HVLab* data acquisition and analysis system via 100-Hz anti-aliasing filters. The acquired signals were low pass filtered at 40 Hz using a 6-pole zero-phase Butterworth filter.

At each frequency, the input motions were generated over a range of magnitudes at 20 equally spaced intervals (Table 6). The performance of a seat in response to each motion was characterized using the ratio of the vibration dose value (VDV, see Eq. (10)) on the seat load to that recorded at the seat base. The VDV was calculated for each motion using the ISO 2631-1 [23] W_k frequency weighting. The frequency weighting was applied using a digital filter that included

the effects of phase:

$$VDV = \left[\int_{t=0}^{t=T} a_w^4(t)\,\mathrm{d}t\right]^{0.25}, \tag{10}$$

where a_w is the W_k frequency-weighted acceleration.

4.2. Simulations

The acceleration time history recorded at the base of the seat was used as the input to the models. The predicted acceleration of the load mass was used to calculate a predicted VDV for comparison with the laboratory measurements.

Identical predicted and measured SEAT values (Eq. (11)) would indicate that the severity of the vibration, expressed in terms of the VDV, was identical but it would not necessarily indicate that the model was predicting the same motion for the seat and the load:

$$SEAT = \frac{VDV_{seat\_surface}}{VDV_{seat\_base}} \times 100. \tag{11}$$

The normalized r.m.s. difference between the predicted and measured load mass acceleration, as defined by Eq. (12), was also calculated to give an alternative indication of the accuracy of predicting the acceleration waveform of the load mass:

$$e = \frac{[\int_{t=0}^{T}(a_{predicted}(t) - a_{measured}(t))^2\,\mathrm{d}t]^{1/2}}{[\int_{t=0}^{T} a_{measured}^2(t)\,\mathrm{d}t]^{1/2}}. \tag{12}$$

5. Results

The VDV on the seat load predicted from the models, compared with the laboratory measurements, is shown for all investigated frequencies of the test motion in Fig. 11. The corresponding r.m.s. errors between the predicted and measured seat load accelerations are shown in Fig. 12, where an error of zero would indicate an exact match between the predicted and measured time histories.

The median absolute difference between the measured and predicted seat surface VDVs for situations without end-stop impacts was 5.9% (inter-quartile range, IQR, 14.3%) of the measured value for the lumped parameter model and 5.4% (IQR 6.6%) of the measured value for the Bouc–Wen model. The median absolute difference for all test conditions was 13.8% (IQR 17.3%) of the measured value for the lumped parameter model and 9.5% (IQR 22.1%) of the measured value for the Bouc–Wen model.

For conditions without end-stop impacts, the median r.m.s. error between the measured and predicted results (i.e., as defined by Eq. (12)) was 0.23 (IQR 0.15) for the lumped parameter model and 0.33 (IQR 0.08) for the Bouc–Wen model. Over all test conditions, the median r.m.s. error was 0.30 (IQR 0.16) for the lumped parameter model and 0.32 (IQR 0.08) for the Bouc–Wen model.

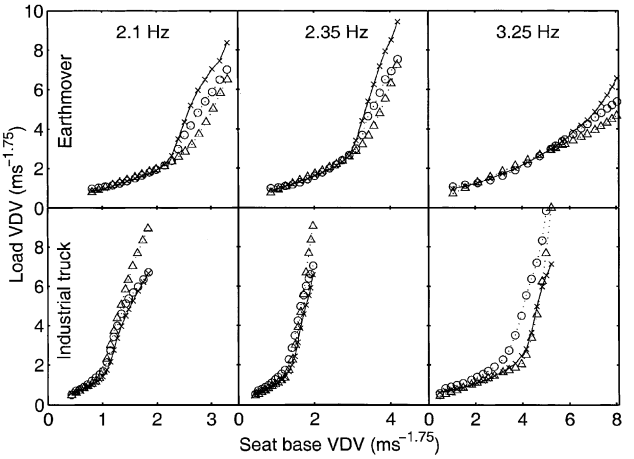

Fig. 11. Predicted and measured vibration dose values for both seats at 2.1, 2.35 and 3.25 Hz inputs (×—laboratory measurements, ○—lumped parameter model, Δ—Bouc–Wen model, note the *x*-axis scaling).

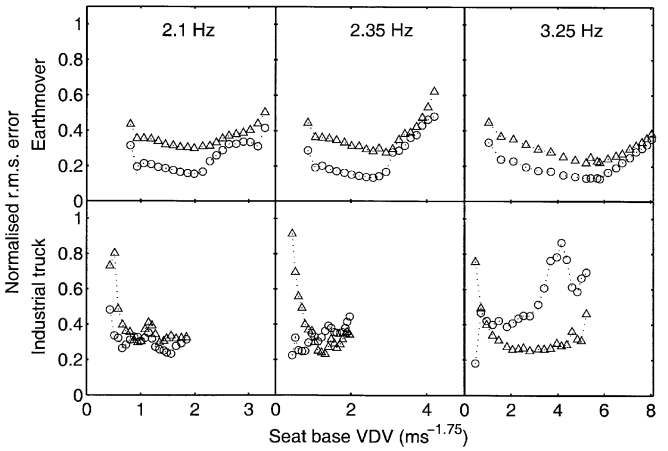

Fig. 12. Normalized r.m.s. error for both seats at 2.1, 2.35 and 3.25 Hz inputs (○—lumped parameter model, Δ—Bouc–Wen model, note the *x*-axis scaling).

Both models underestimated the VDV on the earthmover seat in situations involving end-stop impacts: the r.m.s. error increased with increasing input magnitude (i.e. with increased severity of end-stop impact). Examination of the acceleration time histories showed that the models provided reasonable predictions of the acceleration due to the bottom end-stop impact, but did not predict a sufficiently severe upwards acceleration as the load returned to the seat after a top-stop impact.

With the industrial truck seat, the rate of increase of seat surface VDV with increasing vibration magnitude showed a tendency to decrease at high magnitudes. The lumped parameter model showed this trend while the Bouc–Wen model did not.

6. Strengths and weaknesses of the two models

The advantage of describing the response of a seat by parameters representing individual components, as in the lumped parameter model, is that the effect of each component on the seat performance can be determined and its behaviour understood. This gives a seat manufacturer the potential to estimate the effect of changing the characteristics of a seat component prior to testing. The problems are that a suitable mathematical model must be generated and suitable values for all parameters in the model must be obtained for every seat component affecting the seat dynamic performance. For some components of the seat, such as the suspension damping and friction, the appropriate values may be difficult to determine accurately.

The advantage of the Bouc–Wen approach is that the influence of one component of an existing seat can be examined without the need to dismantle the seat and measure the characteristics of many components. This model was initially developed to investigate the effect of the end-stop buffers and used the Bouc–Wen model to provide a single representation all the combined non-linear effects coming from friction, the damper, different clearances and the seat cushion. Improvements to the model are possible and a particular component of the seat suspension could be represented mathematically and added to the whole model. The problems of this approach are those of identification and optimization methods: the choice of initial parameters, the uniqueness of the final set of parameters, convergence of estimates, the selection of algorithms and numerical methods. Furthermore, the global approach does not provide an opportunity to link physical phenomena with the model parameters, except for the spring stiffness and the stiffness of the bottom buffers.

The prediction of the shocks caused by the top end-stop buffers was not complete for either model, especially when the inert mass lifted free of the seat cushion and returned (this was the case with the earthmover seat when severe end-stop impacts occurred). The Bouc–Wen model introduced an 'equivalent end-stop buffer' to describe the acceleration time histories during top end-stop buffer impacts, but assumed the load did not lift off the seat cushion. The lumped parameter model was able to account for the load lifting off from the seat during top-stop impacts by limiting the overall cushion force acting downwards on the load to 1 g. However, this model had the same difficulties when the load rebounded on the seat cushion.

The lumped parameter model seems to be useful in that it offers a practical method for assisting the design new seats or the modification of existing seats. The Bouc–Wen model may be best suited to situations were the seat is a part of a more complex model of the vehicle. In such situations, a description of the global behaviour of a seat is sufficient and a precise model of a specific component part is not necessary. This may be attractive for studies focused on predicting the vibration exposure of a seated person, or for optimizing the end-stop buffers. The seat is represented as a non-linear filter, providing a transfer function between the vehicle motion and the excitation of the human body.

7. Conclusions

Both a lumped parameter model and a Bouc–Wen model can provide useful predictions of the responses of suspension seats to transient inputs. For extreme motions, both models would be

improved by refining the response of the seat cushion and the cushion–load interface to motions arising from impacts with the top end-stops. Improved characterization of seat suspension components (especially the damper coefficients) is required for the lumped parameter model to provide good predictions without the optimization of model coefficients using experimental data. The Bouc–Wen model requires further development for application to situations where the seat load can rebound on the seat cushion after an impact with the top end-stop buffers.

It is concluded that lumped parameter models can assist seat manufacturers in designing new seats, or modifying existing seats. The Bouc–Wen model is particularly suited to situations where a seat is an input or output to another system. For this application, a description of the global dynamic behaviour of the seat is sufficient.

Appendix A. Parameter values used by the lumped parameter model

			Earthmover seat	Industrial truck seat
Load mass (m_1)			58 kg	58 kg
Cushion stiffness (k_c)			92.1 kN/m	170 kN/m
Cushion damping (c_c)			1371 N s/m	1250 N s/m
Suspension moving mass (m_{mm})			27 kg	13.5 kg
Suspension linkage friction			74 N	26 N
Suspension stiffness (k_s)			4.57 kN/m	10.4 kN/m
Suspension damper gas loading stiffness (k_d)			2.3 kN/m	N/A
Horizontal distance between damper mounting points at mid-ride			150 mm	N/A
Vertical distance between damper mounting points at mid-ride			111 mm	N/A
Damper force–velocity characteristic fit coefficients (before adjustment)	Compression	c_1	0	0
		c_2	0	0
		c_3	0	0
		c_4	-107	1.80×10^2
		c_5	6.32×10^3	0
		c_6	0	0
		$\dot{z}_1$	0	0
	Extension	c_1	0	-3.55×10^1
		c_2	0	1.50×10^3
		c_3	0	0
		c_4	6.16×10^1	1.01×10^3
		c_5	1.03×10^4	3.49×10^3
		c_6	0	1.44×10^5
		$\dot{z}_1$	4.5×10^{-2} m/s	2.9×10^{-1} m/s

Free travel between end-stops ($2d$)		64 mm	50 mm
Damper friction in extension (before adjustment)		173 N	30 N
Damper friction in compression (before adjustment)		64 N	8 N
Bottom buffer axial force-deflection characteristic fit coefficients where x is the buffer compression (F_B)	k_5	1.83×10^{11}	3.20×10^{12}
	k_4	-8.57×10^{7}	-8.04×10^{10}
	k_3	-4.45×10^{7}	8.72×10^{8}
	k_2	1.50×10^{6}	-3.86×10^{6}
	k_1	7.63×10^{3}	5.42×10^{4}
Number of bottom buffers		2	2
Horizontal distance between the ends of the linkage arm at mid-ride		295 mm	N/A
Vertical distance between the ends of the linkage arm at mid-ride		150 mm	N/A
Top buffer axial force–deflection characteristic fit coefficients where x is the buffer compression (F_T)	k_5	5.48×10^{15}	0
	k_4	-2.57×10^{4}	8.2×10^{11}
	k_3	2.60×10^{3}	-6.66×10^{9}
	k_2	3.27×10^{7}	2.17×10^{7}
	k_1	1.35×10^{5}	3.98×10^{4}
Number of top buffers		2	2

References

[1] International Organization For Standardization, Agricultural wheeled tractors—operator seat—measurement of transmitted vibration, Draft International Standard ISO/CD 5007, 1999.

[2] International Organization For Standardization, Earth moving machinery—laboratory evaluation of operator seat vibration, International Standard ISO7096, 2000.

[3] European standard, Mechanical vibrations—industrial trucks—laboratory evaluation and specification of operator seat vibration, Final Draft prEN 13490, 2001.

[4] S. Rakheja, A.K.W. Ahmed, S. Sankar, R.B. Bhat, Ride vibration levels at the driver–seat interface, Report prepared by the Concave Research Centre, Department of Mechanical Engineering, Concordia University, Montreal, Quebec, 1987.

[5] G. Gouw, S. Rakheja, S. Sankar, Y. Afework, Increased comfort and safety of drivers of off-highway vehicles using optimal seat suspension, *Journal of Commercial Vehicles* 99 (1990) 541–548.

[6] S. Rakheja, Y. Afework, S. Sankar, An analytical and experimental investigation of the driver–seat–suspension system, *Vehicle System Dynamics* 23 (1994) 501–524.

[7] R. Ranganathan, K. Sriram, Development of a PC-based software for analysis of off-road vehicle seat suspensions, *International Off-Highway & Powerplant Congress & Exposition*, Milwaukee, WI, September 12–14, 1994.

[8] X. Wu, M.J. Griffin, Simulation study of factors influencing the severity of suspension seat end-stop impacts, *Human Response to Vibration Conference*, Silsoe, 19–21 September, 1995.

[9] O.B. Ahmed, J.F. Goupillon, Predicting the ride vibration of an agricultural tractor, *Journal of Terramechanics* 34 (1) (1997) 1–11.

[10] V.K. Tewari, N. Prasad, Three-DOF modelling of tractor seat–operator system, *Journal of Terramechanics* 36 (4) (1999) 207–219.

[11] T. Gunston, An investigation of suspension seat damping using a theoretical model, *Human Response to Vibration Conference*, Institute of Sound and Vibration Research, Southampton, UK, 13–15 September 2000.
[12] J. Rebelle, Development of a numerical model of seat suspensions to optimise the end-stop buffers, *Human Response to Vibration Conference*, Institute of Sound and Vibration Research, Southampton, UK, 13–15 September 2000.
[13] T.T. Baber, Y.K. Wen, Random vibration of hysteretic degrading systems, *American Society for Civil Engineers, Journal of Engineering Mechanics Division* 107 (EM6) (1981) 1069–1087.
[14] R. Bouc, Modéle mathématique d'hystéresis, *Acustica* 24 (1967) 16–25.
[15] L. Wei, M.J. Griffin, Influence of contact area, vibration magnitude and static force on the dynamic stiffness of polyurethane foam, *Human Response to Vibration Conference*, Institute of Sound and Vibration Research, Southampton, UK, 17–19 September 1997.
[16] L. Wei, M.J. Griffin, The prediction of seat transmissibility from measures of seat impedance, *Journal of Sound and Vibration* 214 (1998) 121–137.
[17] T. Gunston, A method of estimating the damper characteristics for a suspension seat dynamic model, *Human Responses to Vibration Conference*, Centre for Human Sciences, QinetiQ, Farnborough, UK, 12–14 September 2001.
[18] Y.K. Wen, Method for random vibration of hysteresis systems, *Journal of Engineering Mechanics Division* 102 (EM2) (1976) 249–265.
[19] J.A. Nelder, R. Mead, A simplex method for function minimization, *Computer Journal* 7 (1965) 308–313.
[20] J.J. Moré, The Levenberg–Marquardt algorithm: implementation and theory, in: G.A. Watson (Ed.), *Lecture Notes in Mathematics*, Vol. 630, Springer, Berlin, 1977.
[21] T. Gunston, The definition of suitable input motions for testing suspension seat end-stop impact performance, *Human Response to Vibration Conference*, Dunton, Essex, UK, 22–24 September 1999.
[22] International Organization For Standardization, Earth moving machinery, and tractors for agriculture and forestry—seat index point, International Standard ISO 5353, 1999.
[23] International Organization For Standardization, Mechanical vibration and shock—evaluation of human exposure to whole-body vibration—Part 1; general requirements, International Standard 2631-1, 1997.